Scientific Research Publishing

Advances in Materials Physics and Chemistry, 2023, 13, 59-76
https://www.scirp.org/journal/ampc
ISSN Online: 2162-5328
ISSN Print: 2162-531X

Preparation and Study of Carbide-SiAlON Composite in SiC-SiAlON-Al_2O_3 System

Zviad Kovziridze, Natela Nizharadze, Gulnazi Tabatadze, Marina Kapanadze, Nazi Kutsiava, Tsira Danelia, Nino Darakhvelidze, Maia Balakhashvili, Salome Gvazava

Institute of Bionanoceramics and Nanocomposites Technology, Georgian Technical University, Tbilisi, Georgia
Email: kowsiri@gtu.ge

How to cite this paper: Kovziridze, Z., Nizharadze, N., Tabatadze, G., Kapanadze, M., Kutsiava, N., Danelia, T., Darakhvelidze, N., Balakhashvili, M. and Gvazava, S. (2023) Preparation and Study of Carbide-SiAlON Composite in SiC-SiAlON-Al_2O_3 System. *Advances in Materials Physics and Chemistry*, **13**, 59-76.
https://doi.org/10.4236/ampc.2023.135005

Received: March 8, 2023
Accepted: May 13, 2023
Published: May 16, 2023

Abstract

Goal: Synthesis of SiAlON by reaction coating method using aluminosilicate natural raw material geopolymer (kaolin), corundum and silicon carbide and on its basis obtaining a composite with high physical and technical properties by hot pressing for use in armor and rocket technology. For the intensification of SiAlON formation and sintering processes, the influence of various additives was studied, such as: aluminum powder, elemental silicon, yttrium and magnesium oxides. **Method:** A SiAlON-containing composite with an open porosity of 15% - 16% was obtained by the metallothermic process and the method of reactive annealing in nitrogen. The resulting material was milled to a dispersion of 1 - 3 μm and hot pressed at 1620˚C to obtain a product with high density and performance properties. We studied the process of SiAlON formation and the microstructure of the composite by X-ray phase, optical and electronmicroscopy analysis methods. **Result:** In the selected composition the β-SiAlON was formed at 1400˚C instead of 1800˚C, which was due to the mutual influence of the initial raw materials: geopolymer kaolin, perlite, corundum, aluminum, silicon, SiC, the development of the process is facilitated by the vitreous dopant perlite (96 glass phase). The use of perlite, which is eutectic with geopolymer at low temperatures, creates a good prerequisite for intensive diffusion processes with other components. **Conclusion:** A SiAlON-containing composite with high physical and technical properties was obtained in the SiC-SiAlON-Al_2O_3 system by the method of reactive sintering and hot pressing, with the following properties: the strength limit in compression is 1940 MPa, and in bending it is 490 MPa. The process of making SiAlON has been studied using X-ray phase and electron microscopy analysis methods. The physical and technical properties of the obtained composite are studied by modern research methods.

Keywords

SiAlON, Composite, Hot Pressing, Microstructure, Phase Composition

1. Introduction

Technical progress is accompanied by the development and improvement of various fields, which in itself is related to the need to create multifunctional materials with new properties. Materials created on the basis of refractory carbides, borides, nitrides and silicides are distinguished by following operational properties: high fire resistance, high heat resistance, corrosion resistance to aggressive media, macro- and micromechanical, specific electrical and thermophysical properties and others [1] [2] [3] [4] [5].

Intensive work is underway to obtain such ceramic composites, which will reveal the properties of both oxygen-free and oxygencontaining compounds. One group of such materials is represented by SiAlON s, which contain silicon, aluminum, oxygen and nitrogen.

SiAlONs (Si-Al-O-N) are solid solutions of variable composition formed on the basis of $Si_3N_4Si_6$-$Al_xO_xN_{8-1}$(x~O/4.2), with partial replacement of silicon atoms with aluminum and nitrogen atoms with oxygen. SiAlONs are characterized by different types of structure [6] [7] [8] [9] [10]: silicon nitride, silicon oxynitride, aluminum nitride and mullite structure [11]-[17].

SiAlON-containing composites are characterized by a number of properties such as high viscosity, strength, thermal resistance, thermal conductivity, fire resistance, corrosion and wear resistance, etc. At the same time, they maintain these properties when working under high temperature conditions. Sialonic materials can be used in the oxidizing area up to 1300˚C, and in the non-oxidizing environment up to 1800˚C [18] [19] [20].

There are different ways of receiving SiAlON [20]-[26], mostly laboratory experiments, as for the industrial methods of obtaining SiAlONs, the information is less compared to laboratory methods. This can be explained by the fact that the obtained product is highly sensitive to the chemical composition of the raw materials and the parameters of the synthesis process. That is why it becomes difficult to predict the phase composition of the acceptable product as a result of the synthesis. Therefore, taking into account and studying all the nuances of making SiAlONs is an urgent task for the development of modern techniques for making new multi-functional materials.

2. Main Part

One of the main goals of the presented work was to obtain a SiAlON-containing (β-SiAlON) composite based on aluminum oxide and silicon carbide. It is known that when making refractory materials based on silicon carbide, the use of SiAlON as a binder is more preferable than oxide. Silicon carbide materials with nitride binders are characterized by high strength, wear resistance and resistance to thermal shocks.

To fulfill this goal, such raw materials were selected, which would allow us to use newly formed components in the process of reactive lubrication. It is known that incorporation of α-Al_2O_3 and AlN into β Si_3N_4 is easier when its structure is not yet fully formed. This is made possible by our selected natural alumino-

silicate raw materials-kaolin, aluminum powder, elemental silicon and their interaction during reactive lubrication in the nitrogen area and the parallel course of the aluminothermic process. Aluminum oxide and silicon carbide were also used as starting materials, magnesium and yttrium oxides and perlite as lubrication activators, which interacts with kaolin and creates good conditions for intensive diffusion processes at low temperatures.

When selecting the mixtures, we aimed to determine the influence of each component in the process of SiAlON formation.

At the same time, to obtain the composite, we took into account the content of silicon in β-SiAlON, and the composition of the CH-6 mixture was chosen in such a way that the process was directed in the direction of obtaining this type of SiAlON.

The samples were prepared using the same technology discussed in our papers [27] [28] [29].

To characterize the structure of the physical phases of the samples, not only X-ray diffraction analysis was used, on DRON 3, but also electron microscopic analysis, which was carried out on an instrument of the Japanese company, OPTON. We also performed X-ray microanalysis on an OXFORD Instrumentals X-max detector.

X-ray structural analysis showed (**Figure 1**) that in the samples baked at 800˚C, which contained only kaolin and aluminum powder, reflexes of aluminum, quartz and silicon were fixed in addition to the ones we introduced: d_{hkl}:

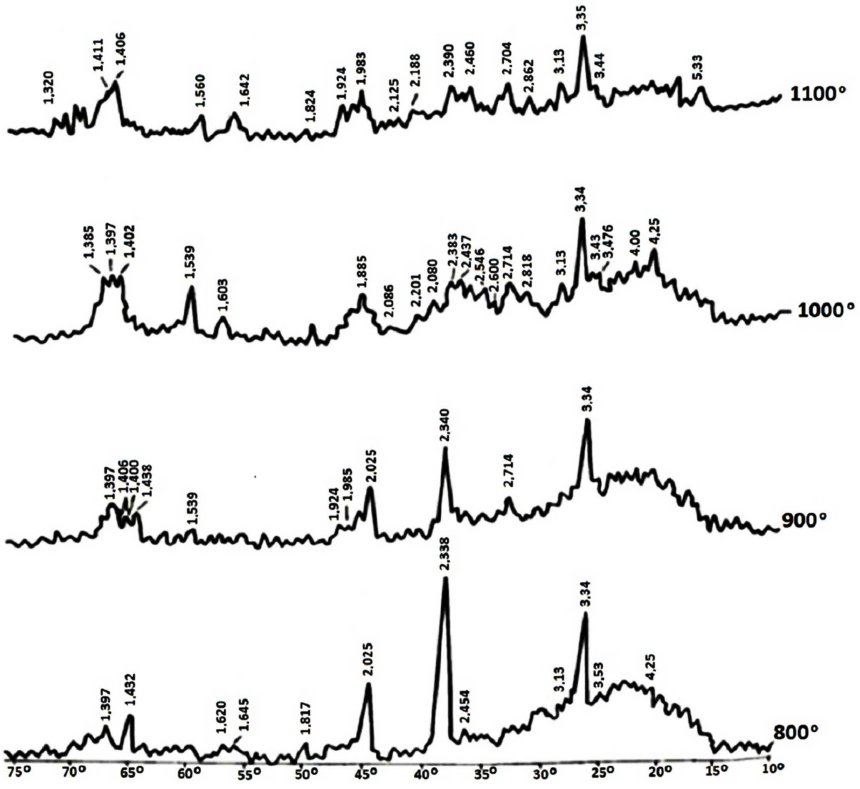

Figure 1. CH-1 X-RAY (800˚C - 1100˚C).

Al—2.338; 2.025; 1.62; 1.432 Å; SI-3.53; 3.13; 2.45; 1.817 Å; SiO_2—3.34; 4.25; 2.454; 1.817 Å.

As a result of the decomposition of kaolinite, silicon oxide was released, and silicon was formed as a result of the alumothermy process according to the following reaction:

$$3SiO_2 + 4Al \rightarrow 2Al_2O_3 + 3Si$$

In the interval of 900˚C - 1000˚C, the peaks of aluminum oxynitride and aluminum nitride appear, and the peaks of aluminum and quartz are significantly reduced, which was caused by reactive and aluminothermic processes in the nitrogen area. 1000˚C d_{hkl}: SiO_2—4.25; 3.34; 2.280; 2.546 Å. Si-3.13; 3.53; 1.817 Å. AlN—2.714; 2.437; 1.402; 1.397 Å. AlON—2.383; 1.985; 1.385 Å (Figure 1).

In the interval of 1100˚C - 1200˚C, aluminum and elemental silicon are no longer fixed, while the intensity of aluminum nitride and aluminum oxynitride peaks increases. Reflexes characteristic of mullite appeared. 1200˚C d_{hkl}: AlN—2.734; 2.700; 2.46; 2.383; 1.548; 1.435; 1.418; 1.334 Å. mullite—5.45; 3.43; 3.395; 2.885; 2.546; 2.295; 2.208; 1.899; 1.990; 1.824; 1.705; 1.530 Å; AlON-1.993 Å; (Figure 2).

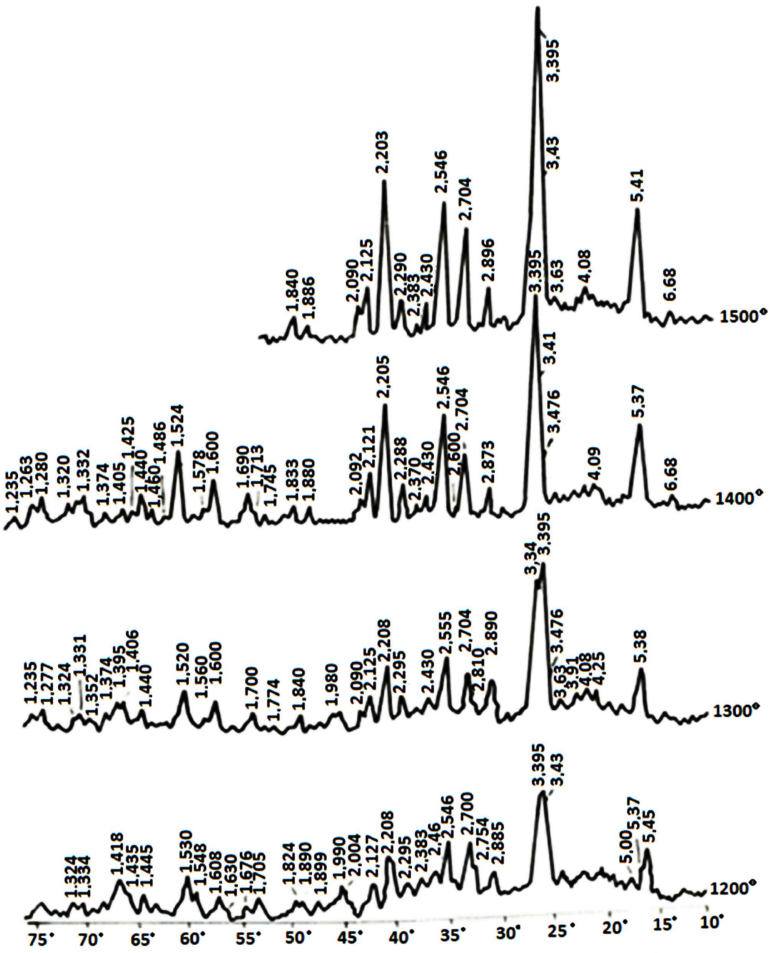

Figure 2. CH-1 X-RAY (1300˚C - 1500˚C).

At 1300˚C - 1500˚C, mullite is the main phase, and silicon nitride is not fixed, which indicates that at 1300˚C x-SiAlON with mullite structure was formed. 1300˚C d_{hkl} mullite 5.38; 3.395; 2.89; 2.704; 2.555; 2.43; 2.29; 2.125; 1.84; 1.700; 1.600; 1.520; 1.44 Å; AlN—2.70 Å.

At 1400˚C - 1500˚C, the peaks of mullite increased significantly, corundum is in the form of traces, silicon nitride reflex appeared $d_{hkl}Si_3N_4$—6.88Å.

In Table 1, X-ray structural analysis of the samples obtained by sintering under the same conditions of the second composition showed a similar result as in the case of the CH-1 composition, while the silicon carbide introduced into the case remains unchanged at all temperatures (Figure 3 and Figure 4). Thus, we can conclude that a composite with a crystalline phase of silicon carbide and X-SiAlON binder has been obtained.

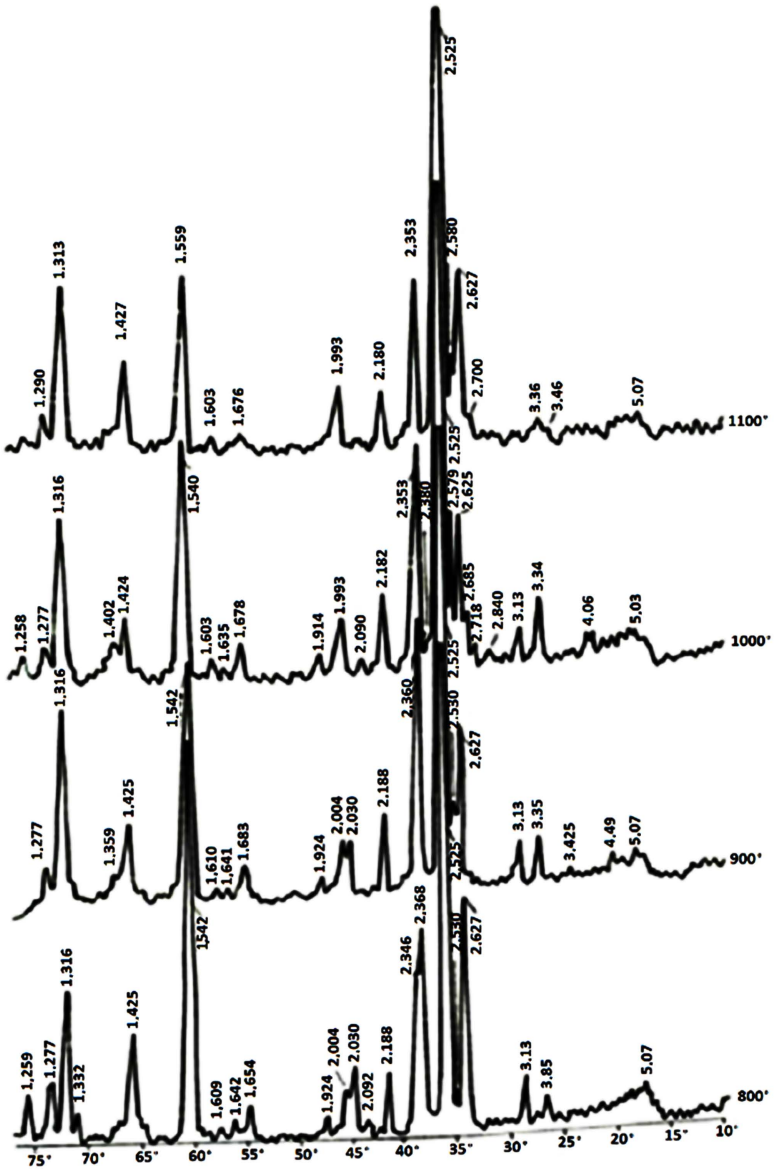

Figure 3. X-RAY of CH-2 composite (800˚C - 1100˚C).

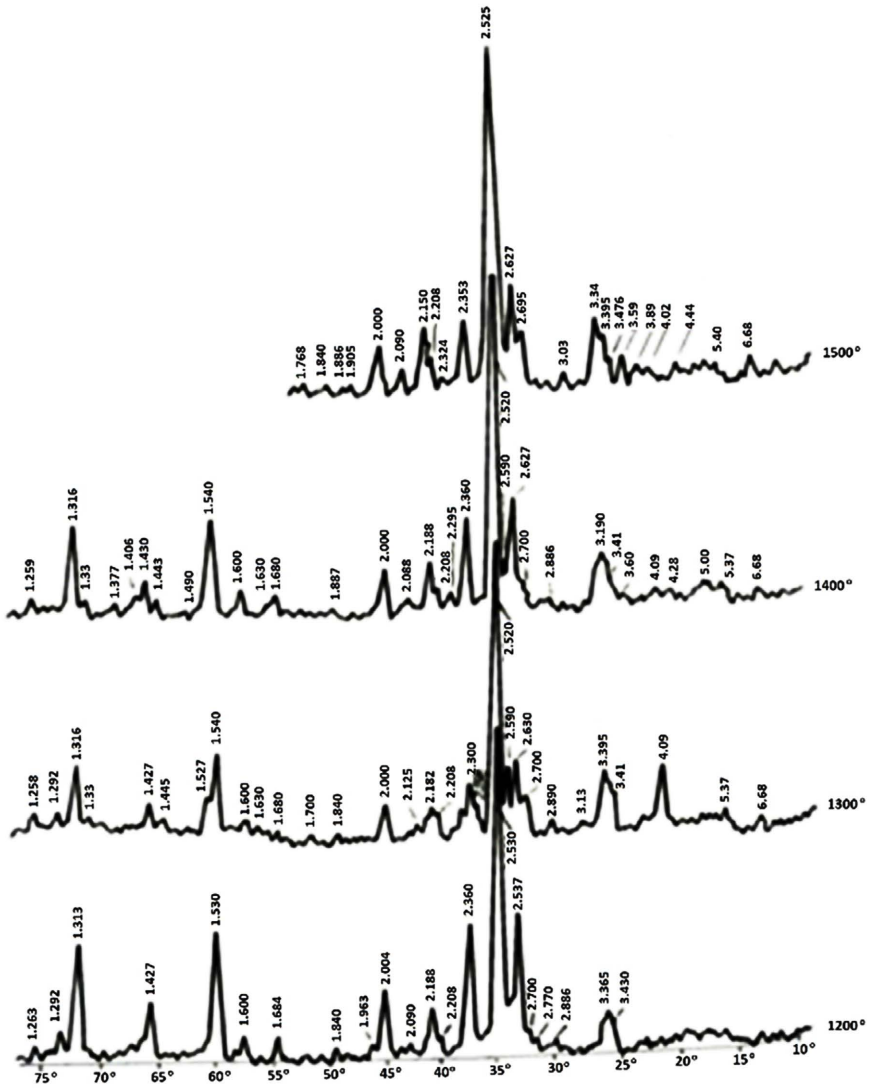

Figure 4. X-RAY of CH-2 composite (1200˚C - 1500˚C).

Table 1. Mixture components.

Number of Composite	Content of Components, wt.%							
	Kaolin	Al	Al_2O_3	SiC	Si	Perlite	Y_2O_3	MgO
CH1	80	20						
CH2	20	10		70				
CH3	20	10	70					
CH6	18.52	18.52	18.52	18.52	20.37	2.78	1.85	0.92

In the samples obtained with the CH-3 composition, the process follows the same scheme as in the case of the previous compositions, while the added *α*-corundum remains unchanged in the material and a composite is obtained with corundum and X-SiAlON binder (Figure 5 and Figure 6).

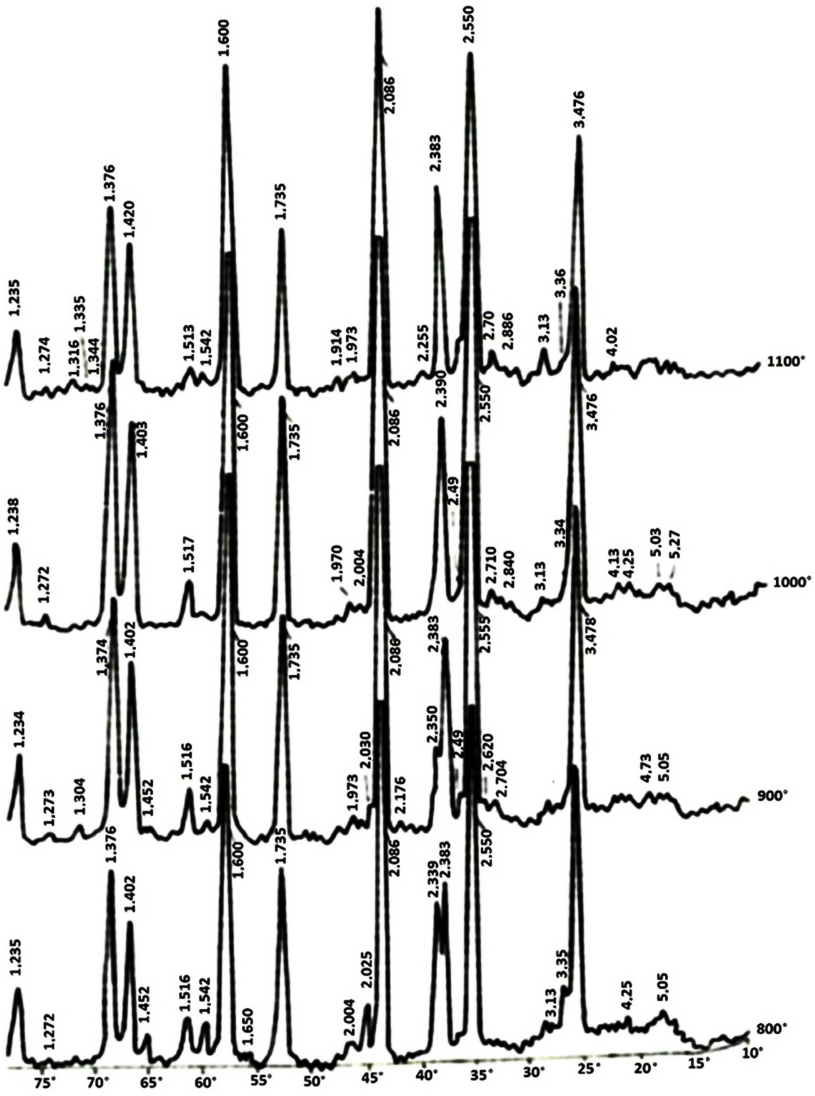

Figure 5. X-ray of CH-3 composite (800˚C - 1100˚C).

In order to obtain the β-SiAlON composite containing silicon carbide and α-corundum, elemental silicon was added to the composition of the chasm and the content of corundum and silicon carbide was reduced. The study of the samples obtained by reactive annealing, nitrogen area and aluminothermic method at 1500˚C showed that the obtained composite consists mainly of β-SiAlON, silicon carbide and α-corundum (**Figure 7**), and the physical and technical data are presented in **Table 2**.

It can be seen from **Table 2** and the electron microscopy analysis (**Figure 8**) that the samples are porous, and as for the phase composition, it corresponds to the X-ray structural analysis data.

In order to obtain a low porosity and dense product, the synthesized CH-6 composite material was crushed and pressed by the hot pressing method at 1620˚C under a pressure of 30 MPa, the vacuum was 10^{-3} Pa. The mode of hot pressing is presented in **Figure 9**.

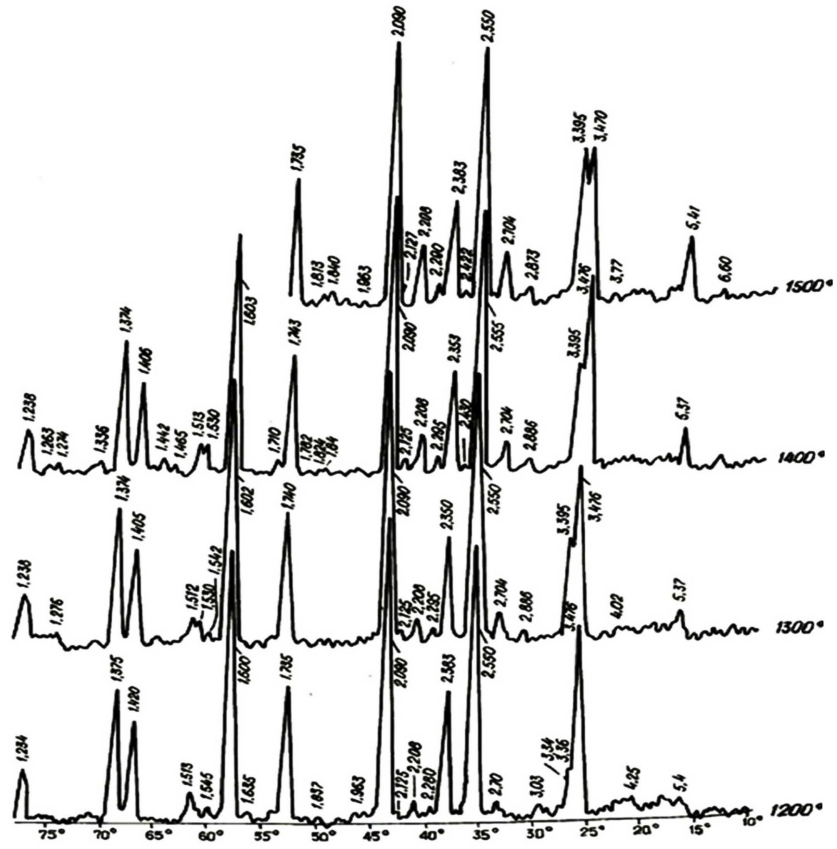

Figure 6. X-RAY of CH-3 composite (1200˚C - 1500˚C).

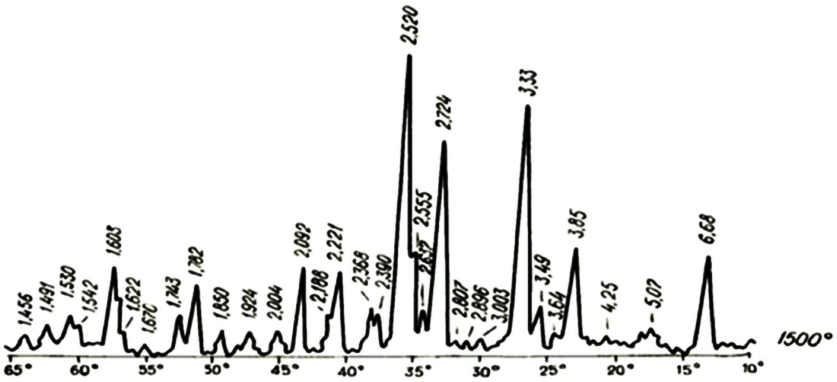

Figure 7. X-RAY of CH-6 composite (1500˚C).

Table 2. Physical and technical characteristics of the samples obtained by reactive annealing, in the nitrogen area and by the alumothermic method at 1500˚C.

Composite	Open Porosity W, %	Compressive strength $\sigma_{c.\,MPa}$	density, P, g/cm$^{3/}$	Chemical resistivity, %	
CH-1	16.2	230	2.28	water	acid
CH-2	15.5	245	2.80	99.41	99.16
CH-3	16.0	240	3.2	99.36	99.15
CH-6	15.0	256	2.25	99.82	99.20

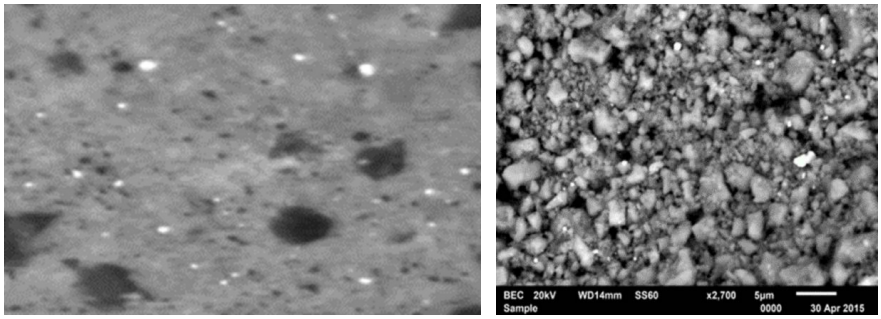

(a) (b)

Figure 8. CH-6 1500˚C; (a) X-500; (b) X-2700.

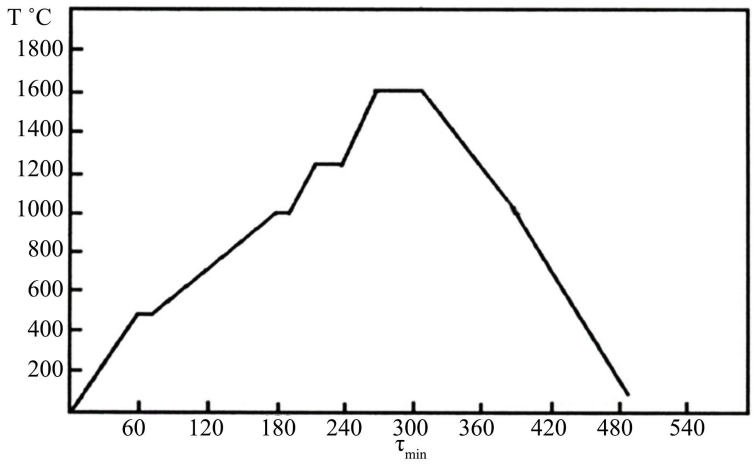

Figure 9. Temperature mode of hot pressing.

We studied the physical and technical properties of the hot-pressed samples (**Table 3**), from which it can be seen that an almost non-porous (0.5% open porosity) material with high mechanical properties was obtained: the strength limit in compression is 1940 MPa, and in bending is 490 MPa. What is more important in the perspective of using this composite.

As a result of the X-ray structural analysis and electron-microscopic study of the hot-pressed samples, it was determined that the phase composition has not changed and the composite is β-SiAlON d_{hkl}: 7.95; 5.63; 3.85; 3.65; 2.520; in the matrix 2.19 of silicon carbide d_{hkl}: 2.63; 2.370; 2.19; 2.014; and α-corundum d_{hkl}: 3.49; 2.52; 2.36; 2.090 crystalline phases (**Figure 10** and **Figure 11**).

We also performed micro-X-ray spectral analysis on the research samples on the OXFORD instrumentals detector X-max., several points were probed on the surface of the CH-6 composite sample, by means of which the general composition of the elements containing the composite was investigated in each sampled point. The results are presented in (**Figure 12**).

As a result of the research, it can be seen that the percentage content of elements confirms the presence of SiAlON, silicon carbide and corundum in the composite, which was confirmed above by the results of both X-ray phase and electronic-structural analyses.

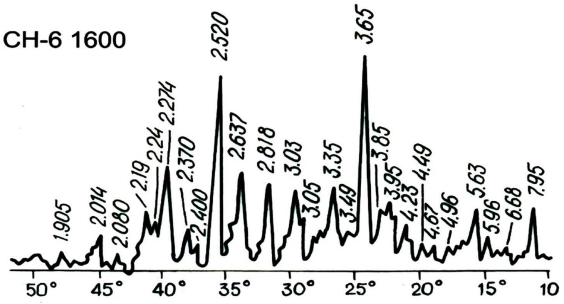

Figure 10. X-ray image of CH-6 composite hot pressed at 1620˚C.

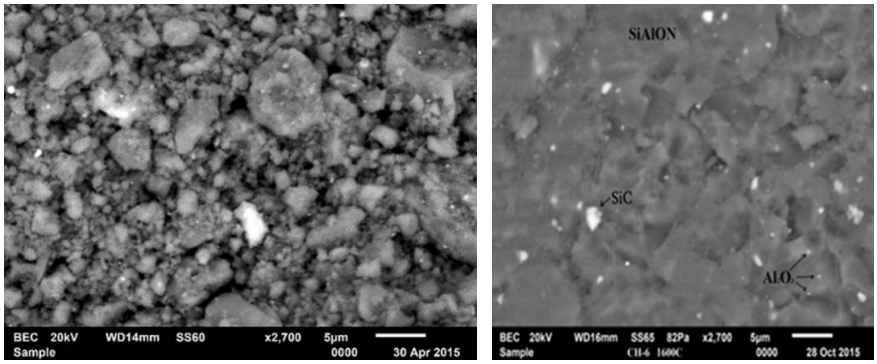

Figure 11. Electron microscopy image of CH-6 composite hot pressed at 1620˚C.

Table 3. Physical and technical indicators of hot pressed CH-6 composite at 1620˚C.

Composite	Open Porosity W, %	General porosity, П, %	density, P, g/cm^3	Thermal expansion Coefficient, α, 10^{-6}˚C-(20 - 700^0)	Fire resistivity, ˚C	Compressive strength $\sigma_{c.\ MPa}$	Bending stress limit, $\sigma_{b.\ MPa}$
CH-6	<0.5	3.95	2.97	3.15	>1770	1940	490

To determine the dynamic microelasticity and modulus of elasticity of the obtained CH-6 composite, we used a modern, dynamic ultra microelasticity tester DUH-211S that meets the requirements of the international standard ISO-14577. The method allows determining the average static viscosity HV based on the size of the indenter's imprint, and the dynamic micro viscosity DHV based on the load applied to the indenter and the depth of its penetration into the material. The advantage of the dynamic method over the static method is that it includes both plastic and elastic components and does not depend on the in homogeneity of the elastic recovery. The test was carried out under different load conditions. The measurement results are given in Table 4 and Table 5, Figure 13 and Figure 14. The average dynamic viscosity of the studied composite is 1029.366, static viscosity is 11.40, and the modulus of elasticity is 199 GPa (at 200 g load), DHV-11045.369 at 100 g load, respectively; HV-11.54; Eit-203, which is a fairly high indicator of the load on the indenter, did not cause a significant difference in the parameter values.

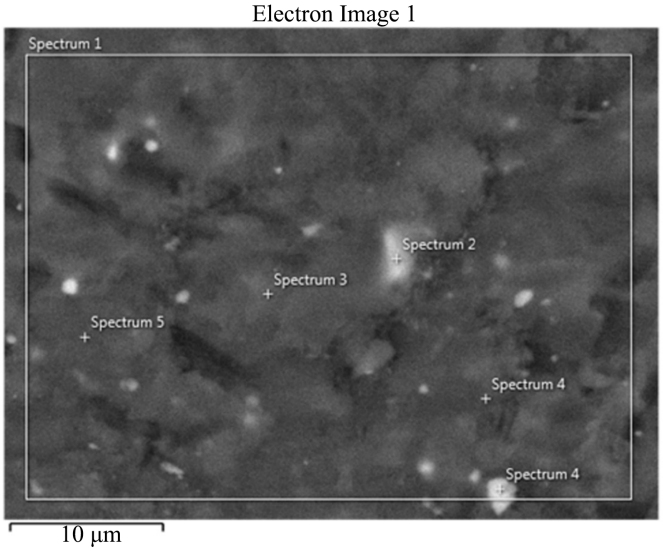
Electron Image 1
Spectrum 1
Spectrum 2
Spectrum 3
Spectrum 5
Spectrum 4
Spectrum 4
10 µm

(a)

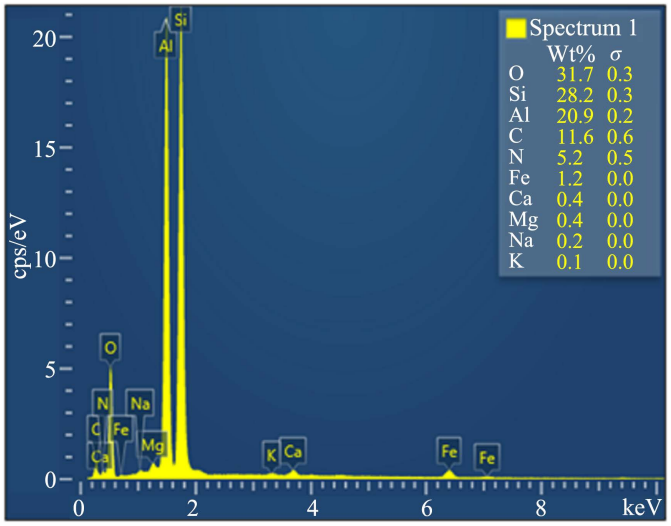
Spectrum 1
Wt% σ
O 31.7 0.3
Si 28.2 0.3
Al 20.9 0.2
C 11.6 0.6
N 5.2 0.5
Fe 1.2 0.0
Ca 0.4 0.0
Mg 0.4 0.0
Na 0.2 0.0
K 0.1 0.0
cps/eV
keV

(b)

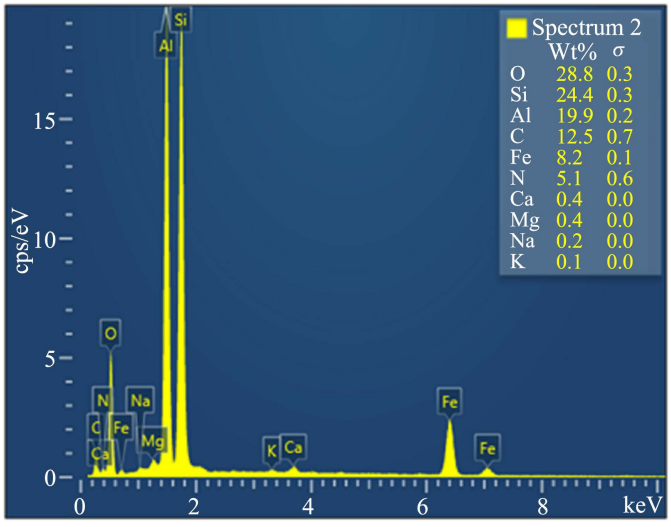
Spectrum 2
Wt% σ
O 28.8 0.3
Si 24.4 0.3
Al 19.9 0.2
C 12.5 0.7
Fe 8.2 0.1
N 5.1 0.6
Ca 0.4 0.0
Mg 0.4 0.0
Na 0.2 0.0
K 0.1 0.0
cps/eV
keV

(c)

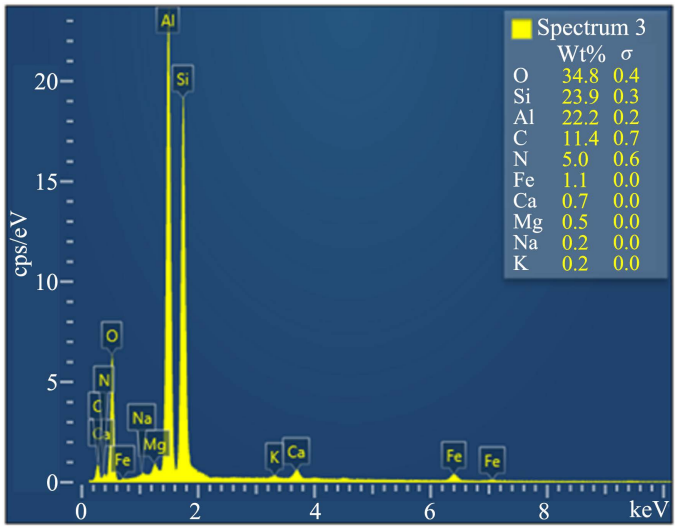
Spectrum 3
Wt% σ
O 34.8 0.4
Si 23.9 0.3
Al 22.2 0.2
C 11.4 0.7
N 5.0 0.6
Fe 1.1 0.0
Ca 0.7 0.0
Mg 0.5 0.0
Na 0.2 0.0
K 0.2 0.0
cps/eV
keV

(d)

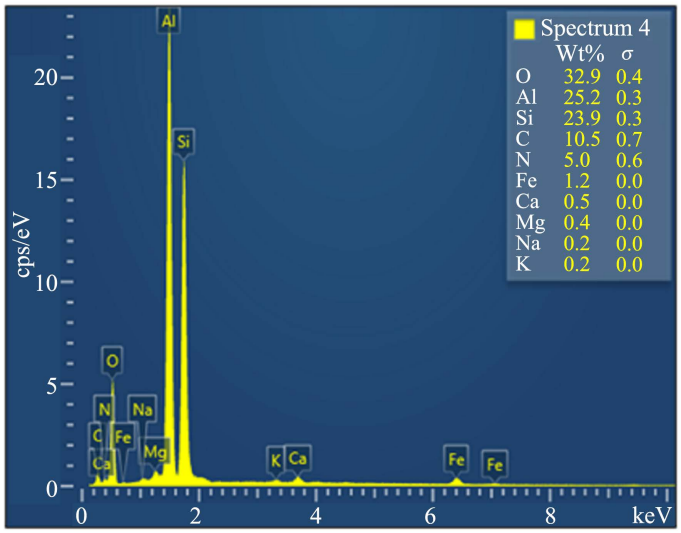
Spectrum 4
Wt% σ
O 32.9 0.4
Al 25.2 0.3
Si 23.9 0.3
C 10.5 0.7
N 5.0 0.6
Fe 1.2 0.0
Ca 0.5 0.0
Mg 0.4 0.0
Na 0.2 0.0
K 0.2 0.0
cps/eV
keV

(e)

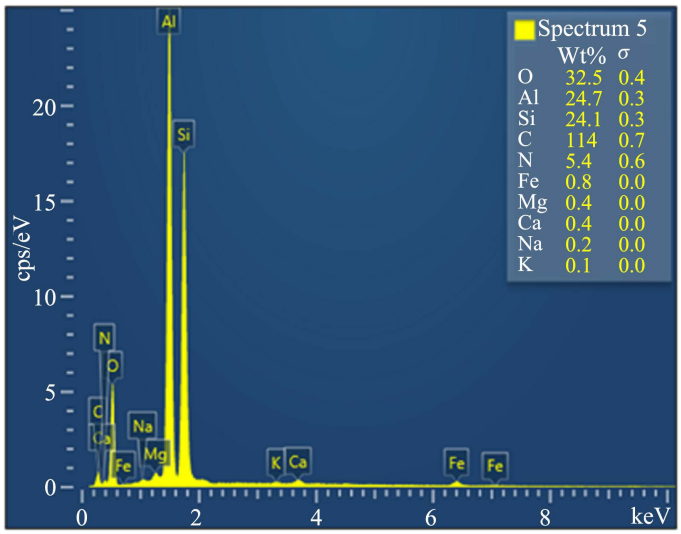
Spectrum 5
Wt% σ
O 32.5 0.4
Al 24.7 0.3
Si 24.1 0.3
C 114 0.7
N 5.4 0.6
Fe 0.8 0.0
Mg 0.4 0.0
Ca 0.4 0.0
Na 0.2 0.0
K 0.1 0.0
cps/eV
keV

(f)

Result Type	Weight %				
Spectrum Label	Spectrum 5	Spectrum 1	Spectrum 2	Spectrum 3	Spectrum 4
C	11.41	11.61	12.52	11.41	10.49
N	5.37	5.22	5.12	4.97	5.01
O	32.52	31.67	28.80	34.78	32.90
Na	0.23	0.20	0.23	0.20	0.20
Mg	0.38	0.38	0.37	0.54	0.44
Al	24.71	20.92	19.88	22.18	25.19
Si	24.11	28.21	24.36	23.95	23.86
K	0.14	0.14	0.14	0.19	0.16
Ca	0.36	0.42	0.38	0.70	0.51
Fe	0.77	1.24	8.20	1.09	1.24
Total	100.00	100.00	100.00	100.00	100.00

Statistics	C	N	O	Na	Mg	Al	Si	K	Ca	Fe
Max	12.52	5.37	34.78	0.23	0.54	25.19	28.21	0.19	0.70	8.20
Min	10.49	4.97	28.80	0.20	0.37	19.88	23.86	0.14	0.36	0.77
Average	11.49	5.14	32.13	0.21	0.42	22.58	24.90	0.15	0.47	2.51
Standard Deviation	0.72	0.16	2.18	0.01	0.07	2.32	1.86	0.02	0.14	3.19

(g)

Figure 12. Results of micro-spectral analysis of CH-6 composite hot pressed at 1620˚C.

Table 4. Test results—CH6-1600 (200 gr).

Test mode	**Load-unload**	**Sample No. CH6-1600**	
Sample name	CH6-1620	Minimum force	1.96 [mN]
Test force	200 [gr]	Hold time at load	5 [sec]
Loading speed	1.0 (70.0670 [mN/sec])	Test count	9
Hold time at unload	3 [sec]	Parameter	20
Comment	20.11.15. CH6-1620-matrix		
Poisson's ratio	0.250		
Indenter type	Vickers		

SEQ	**Fmax**	**hmax**	**DHV-1**	**Eit**	**Length**	**HV**	**Dataname**
	[mN]	[um]		GPa	[um]	GPa	
1	1908.95	3.0142	1047.406	209	17.398	11.92	CH6-1600 (1900) (1)
2	1908.23	3.0219	1041.627	200	17.693	11.52	CH6-1600 (1900) (4)
3	1907.52	3.0035	1054.060	201	16.816	12.75	CH6-1600 (1900) (7)
4	1908.23	3.1456	961.333	191	18.936	10.06	CH6-1600 (1900) (8)
5	1908.95	3.0214	1042.405	195	18.349	10.72	CH6-1600 (1900) (9)
Average	1908.38	3.0413	1029.366	199	17.838	11.40	

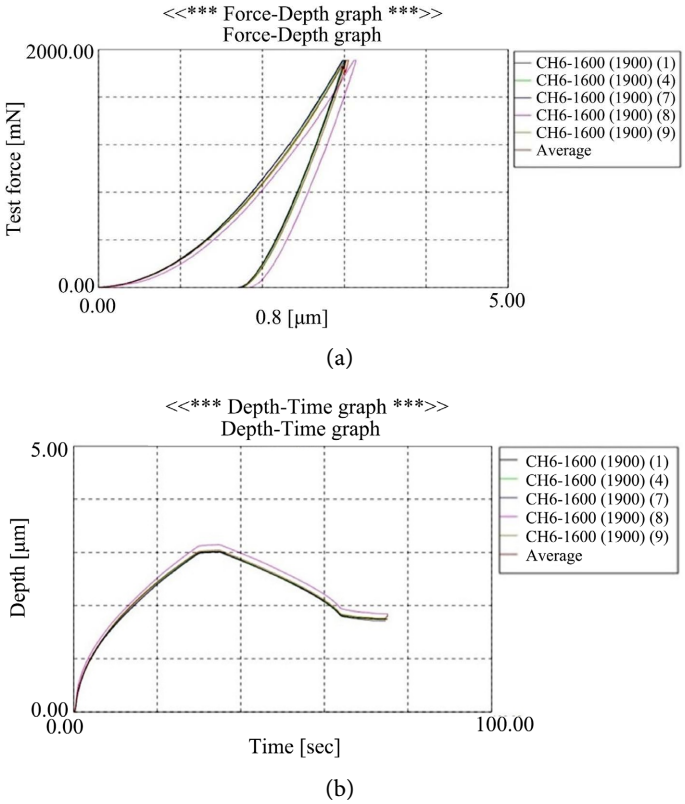

Figure 13. Load-unload curve (200 g) (a) Load force on the indenter; (b) Depth of penetration of the indenter into the material.

Table 5. Test results—CH6-1600 (100 gr).

Test mode	Load-unload	SampleNo. CH6-1600#1	
Sample name	CH6-1620	Minimumforce	1.96 [mN]
Test force	100 [gr]	Holdtimeatload	5 [sec]
Loading speed	1.0 (70.0670 [mN/sec])	Testcount	7
Hold time at unload	3 [sec]	Parameter	20
Comment	20.11.15. CH6-1620		
Poisson's ratio	0.250		
Indenter type	Vickers		

SEQ	Fmax	hmax	DHV-1	Eit	Length	HV	Dataname
	[mN]	[um]		GPa	[um]	GPa	
1	1006.17	2.1999	1036.372	200	13.159	10.98	CH6-1600 (1000) (1)
2	1010.12	2.2287	1013.712	193	12.428	12.36	CH6-1600 (1000) (2)
3	1005.82	2.1582	1076.444	213	12.866	11.49	CH6-1600 (1000) (3)
4	1007.07	2.1779	1058.338	207	13.084	11.12	CH6-1600 (1000) (5)
5	1006.89	2.1948	1041.979	199	12.719	11.77	CH6-1600 (1000) (7)
Average	1007.22	2.1919	1045.369	203	12.851	11.54	

Figure 15 shows the impression of the indenter. As can be seen from the image, the boundaries of the print are sharp and there are cracks of equal size in the corners, which indicates the uniformity and high relative density of the composite.

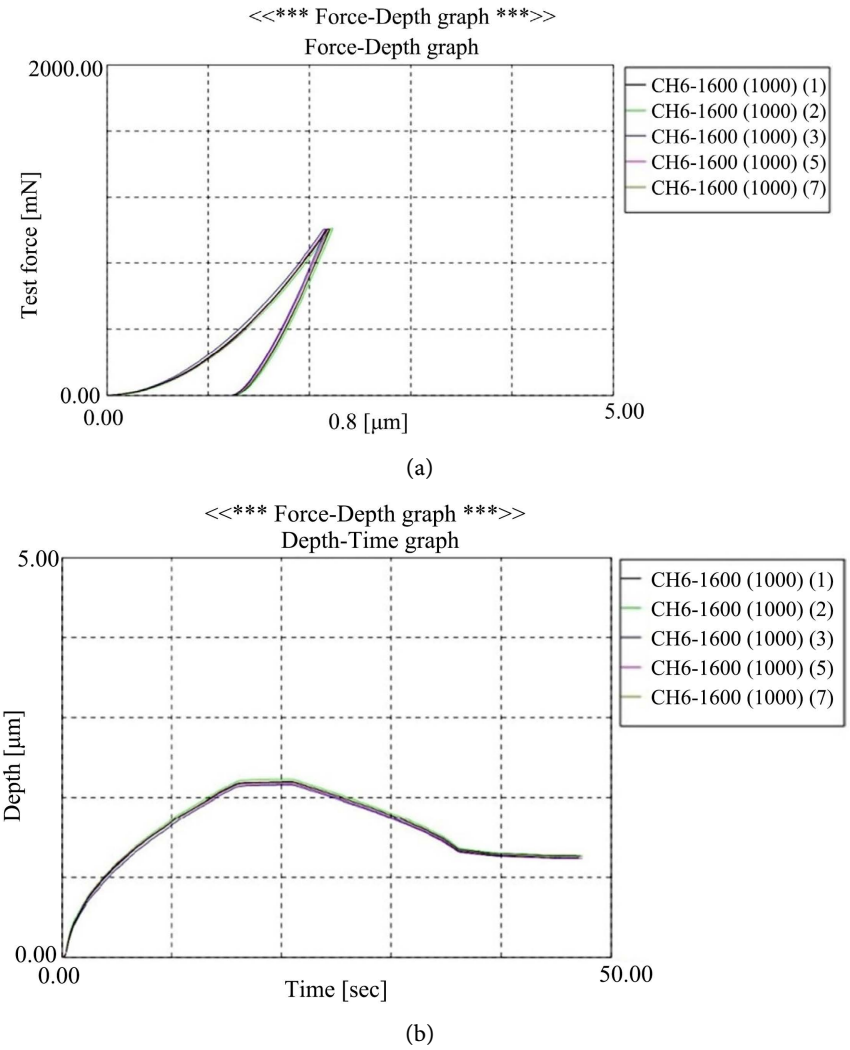

Figure 14. Load-unload curves (100 g) (a) Load force on the indenter; (b) depth of penetration of the indenter into the material.

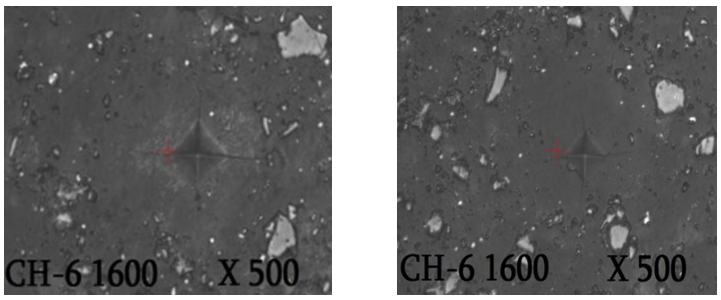

(a) (b)

Figure 15. Impression taken in SiAlON matrix, load (a) 200 g; (b) 100 g.

3. Conclusion

In this way, using aluminosilicate natural raw materials kaolin and perlite, aluminum powder and elemental silicon at 1500˚C, SiAlON was synthesized by the reactive coating method, And on the basis of SiAlON synthesized by hot pressure at 1620˚C, a composite with high physical-technical characteristics (σ_c. = 1940 MPa; σ_b. = 490 MPa) with silicon carbide and corundum crystal phase was obtained, which can be used in such a field of equipment as armored equipment, as well as the high fire resistance, thermal and chemical stability indicators of the obtained composite (Table 2) allow it to be used for work in conditions of high temperatures and aggressive media.

Acknowledgment

We express our gratitude to Shota Rustaveli Georgian National Science Foundation. The work is done with the grant of the Foundation FR-21-1413 Grant 2022.

Conflicts of Interest

The authors declare no conflicts of interest regarding the publication of this paper.

References

[1] Kovziridze, Z., Aneli, J., Nijaradze, N. and Tabatadze, G. (2017) Ceramic and Polymer Composites. Monograph. Lambert Academic Publishing, London, 119-209.

[2] (2018) Properties and Applications of Sialons—A Comprehensive Guide. https://www.azom.com/article.aspx?ArticleID=15727

[3] Wang, L., He, C. and Wu, J. (1989) Oxidation of Sintered Silicon Nitride Materials. Ceramic Materials and Composite Engineering. *Proceedings of the International Symposium*, Las Vegas, Westerville, Ohio, 27-30 November 1988, 604-611.

[4] Zheng, G., Zhao, J., Gao, Z. and Cao, Q. (2012) Cutting Performance and Wear Mechanisms at SIAlON-Si_3N_4 Graded Nano-Composite Ceramic Cutting Tools. *The International Journal of Advanced Manufacturing Technology*, **58**, 19-38. https://doi.org/10.1007/s00170-011-3379-2

[5] Riley, F.L. (2000) Silicon Nitride and Related Materials. *Journal of the American Ceramic Society*, **83**, 10-30. https://doi.org/10.1111/j.1151-2916.2000.tb01182.x

[6] Zabolotskii, A.V., Dolgushev, N.V. and Suvorov, S.A. (2002) Thermodynamic Parameters of β-Sialon. *Inorganic Materials*, **38**, 224-226.

[7] Ekström, T., Käll, P.O., Nygren, M. and Olsson, P.O. (1989) Dense Single-Phase β-Sialon Ceramics by Glass-Encapsulated Hot Isostatic Pressing. *Journal of Materials Science*, **24**, 1853-1862. https://doi.org/10.1007/BF01105715

[8] Rosenflanz, A. and Chen, I.-W. (1999) Phase Relationships and Stability of α'-SiAlON. *Journal of the American Ceramic Society*, **82**, 25-28. https://doi.org/10.1111/j.1151-2916.1999.tb01869.x

[9] https://www.sciencedirect.com/topics/materials-science/sialon.

[10] Xu, L.H., Cheng, K., Liu, M. and Xu, B. (2007) Method for Preparing SiAlON Ceramic Powder by Using Andalusite. Chinese Patent No. CN100534953C. https://patents.google.com/patent/CN100534953C/en.

[11] Long, G. and Foster, L.M. (1959) Aluminum Nitride, a Refractory for Aluminum to 2000°C. *Journal of the American Ceramic Society*, **42**, 53-59. https://doi.org/10.1111/j.1151-2916.1959.tb14066.x

[12] Geffrey, G.A. and Parri, G.S. (1955) Crystal Structure of Aluminium Nitride. *The Journal of Chemical Physics*, **23**, 406-408. https://doi.org/10.1063/1.1741992

[13] Ishutina, Z.N. (1997) Phase Formation and Properties of Materials in Nanocomposites Based on the Al_2O_3-SiO_2-TiO_2 System: Dissertation for the Degree of Candidate of Chemical Sciences. Saint-Petersburg State Institute of Technology, St. Petersburg, 122.

[14] Schmücker, M. and Schneider, H. (1999) Transformation of X-Phase SiALON to Mullite. *Journal of the American Ceramic Society*, **82**, 1934-1936. https://doi.org/10.1111/j.1151-2916.1999.tb02021.x

[15] Akhmadullina, N.S., Sirotinkin, V.P., Ovsyannikov, N.A., Lysenkov, A.S. and Kargin, Y.F. (2022) High-Temperature Interactions of Silicon-Aluminum Oxynitrides (Sialons) with Sodium Fluoride. *Inorganics*, **10**, Article No. 140. https://doi.org/10.3390/inorganics10090140

[16] Ogbuji, L.U.J.T. (1995) The SiO_2-Si_3N_4 Interface, Part II: O_2 Permeation and Oxidation Reaction. *Journal of the American Ceramic Society*, **78**, 1279-1284. https://doi.org/10.1111/j.1151-2916.1995.tb08482.x

[17] Chukhlomina, L.N., Bolgaru, K.A. and Avramchik, A.N. (2013) SV-Synthesis of Composite Ceramics Based on β-Sialon Using FE-SI-AL Alloy. *Journal Refractory and Technical Ceramics*, 15-19.

[18] Zheng, G., Zhao, J., Gao, Z. and Cao, Q. (2012) Cutting Performance and Wear Mechanisms of Sialon-Si_3N_4 Graded Nano-Composite Ceramic Cutting Tools. *The International Journal of Advanced Manufacturing Technology*, **58**, 19-28. https://doi.org/10.1007/s00170-011-3379-2

[19] Tressler, R.E. (1994) Theory and Experiment in Corrosion of Advanced Ceramics. In: Nickel, K.G., Ed., *Corrosion of Advanced Ceramics. NATO Science Series E*: (*Closed*), Vol. 267, Springer, Dordrecht, 3-23. https://doi.org/10.1007/978-94-011-1182-9_1

[20] Piekarczyk, J., Lis, J. and Bialoskorski, J. (1990) Elastic Properties, Hardness and Indentation Fracture Toughness of β-SiAlONs. *Key Engineering Materials*, **89-91**, 542-546. https://doi.org/10.4028/www.scientific.net/KEM.89-91.541

[21] Barris, G.C. and Hodren, G.M. (1998) Ceramic Production Process. US Patent No. 5851943. https://patents.google.com/patent/US5851943A/en?oq=US+Patent+No.+5851943.

[22] Costa Oliveira, F., Edwards, R., Fordham, R. and De Wit, J. (1994) Factors Limiting the Application of Silicon Nitride Ceramics in Sulphur-Containing Environments of Low Oxygen Potential at High Temperatures. In: Nickel, K.G., Ed., *Corrosion of Advanced Ceramics. NATO Science Series E*: (*closed*), Vol. 267, Springer, Dordrecht, 177-188. https://doi.org/10.1007/978-94-011-1182-9_14

[23] Sialon-Containing Material and Composition for Its Production. http://www.findpatent.ru/patent/237/2378227.html

[24] Shveikin, G.P. and Perelyaev, V.A. (1997) Processing of Mineral and Technogeneous Raw Materials by Carbothermal Reduction. *Russian Chemical Bulletin*, **46**, 219-231. https://doi.org/10.1007/BF02494351

[25] Antsiferov, V.N., Gilev, V.G., Bekker, V.Y. and Filimonova, I.V. (2000) A Study of Sialon Synthesis from Kaolin by Carbothermal Reduction and Simultaneous Nitriding. *Refractories and Industrial Ceramics*, **41**, 338-344. https://doi.org/10.1023/A:1011372820939

[26] Shveikin, G.P., Smol'nikov, Y.A., Timoshchuk, T.A., *et al.* (1999) Abrasive Capacity of Ss'-Sialons Synthesized by Hot Pressing. *Refractories and Industrial Ceramics*, **40**, 196-198. https://doi.org/10.1007/BF02762282

[27] Kovziridze, Z., Nizharadze, N., Tabatadze, G., Darakhvelidze, N., Mestvirishvili, Z., Jalaghonia, N., Jalabadze, N. and Balakhashvili, M. (2022) Preparation and Study of High Temperature Composite in SiC-SiAlON-Al203 System. *Ceramics and Advanced Technologies*, **24**, 15-48.

[28] Kovziridze, Z., Nizharadze, N., Tabatadze, G., Cheishvili, T., Mestvirishvili, Z., Msvildadze, M. and Darakhvelidze, N. (2017) Obtaining a Composite by Metallothermic and Sintering Processes in the Si-SiC-Al Geopolymer System. *Journal of Ceramics and Advanced Technologies*, **19**, 33-52.

[29] Kovziridze, Z., Nizharadze, N., Tabatadze, G., Cheishvili, T., Mestvirishvili, Z., Mshvildadze, M., Nikolaishvili, E. and Darakhvelidze, N. (2014) Obtaining Sialon by Nitroaluminothermic Processes. *Journal of Ceramics and Advanced Technologies*, **2**, 23-32.